

# Broadband Parametric Impedance Matching for Small Antennas Beyond the Bode-Fano Limit

Pedram Loghmannia, *Student Member, IEEE*, Majid Manteghi, *Senior Member, IEEE*

**Abstract**— In this letter, a parametric up-converter is introduced as a wideband impedance matching network for electrically small antennas. The proposed technique can also be applied to any narrowband load. Narrowband loads have a high-quality factor because they store a large amount of energy throughout each cycle while dissipating a limited amount of power. We propose lowering a narrowband load's quality factor by increasing its dissipated power while maintaining the general noise figure of the system. The idea is to use a reactive network that emulates a positive resistor to drain power from the narrowband load. The suggested matching network includes a time-varying reactor (capacitor) which is not only a parametric amplifier but also a low noise element.

**Index Terms**—Bode-Fano bound, Chu's limit, parametric amplifier, small antenna, time-variant antenna, wideband matching.

## I. INTRODUCTION

ELECTRICALLY small antennas (ESAs) are one of the inseparable parts of many RF systems with applications in VHF and UHF transceivers, very low-frequency underwater communications, implanted devices, Internet of Things, and portable devices. At the same time, demands for greater information rates encourage the use of wideband antennas by radio engenders. Wheeler and Chu [1], however, showed that small electrical size and wide instant bandwidth cannot be realized concurrently using LTI methods. In the past, many efforts have been made to transmit high data rate and wideband signals using ESAs and break the Chu's limit [2]. However, on the receiving side, the radio engineers have to trade noise figure with the bandwidth that in modern systems may not be a viable option. In this letter, we introduce an active matching methodology that dramatically increases the instantaneous bandwidth of a narrowband antenna while at the same rate it does not increase the system noise.

Using Linear Time-Invariant (LTI) and lossless matching networks [3], Fano performed comprehensive research to match complicated loads (or sources) to a real impedance. In the case of matching a simple leaky inductor/capacitor to pure resistance, he concluded that the match's bandwidth is bounded by the quality factor of the leaky inductor/capacitor considering a fixed value for the reflection coefficient (return loss).

Recently, parametric devices as nonlinear and/or time-

variant components have regained researchers' attention due to their applications in magnetless nonreciprocal devices [4], low noise active antennas [5], and wideband impedance matching techniques [6, 7]. In [7], the transmission line parameters are temporarily switched to match an RC shunt circuit as a complex load to a pure resistance beyond the Bode-Fano bound. This method, due to its reactive nature, improves noise performance compared to the Non-Foster matching technique [8]. However, its operation is restricted to short pulses because of its time-domain nature.

We used the topology of an up-converter parametric amplifier for Continuous Wave (CW) signals as a broadband matching circuit. A small receiving magnetic antenna is modeled as a voltage source (antenna open circuit voltage) connected to a series RL circuit (antenna reactance, L radiation resistance, R). Together with its tuning capacitor, the antenna model is considered as the input circuit (filter and source) for the up-converter parametric amplifier. The input impedance of the parametric amplifier is then tuned to introduce a positive resistance to the receiving circuit of the small antenna and, as a consequence, its quality factor is decreased.

To demonstrate the idea of our proposed wideband matching technique, we used a straightforward circuit model for ESAs. In addition to measured data in our future works, a more sophisticated model for practical antennas will be explored. This paper is outlined as follows: the principle of the proposed technique is theoretically illustrated in chapter II. The simulation results obtained by the Advanced Design System (ADS) are then used to confirm theoretical outcomes in chapter IV. Finally, our findings are contrasted in section IV with Bode-Fano in order to demonstrate the efficacy of the suggested method.

## II. PRINCIPLES OF THE WIDEBAND MATCHING TECHNIQUE

First, in this section, we review the concept of the up-converter parametric amplifier. The wideband matching method and its noise performance are then given using a simple example.

### A. Review of the Up-Converter Parametric Amplifier

Fig 1 shows the small-signal model for an up-converter parametric amplifier. The series combination of  $L_a$  and  $C_1$  in the input circuit is tuned at  $f_s$  as a bandpass filter, while in the output

circuit,  $C_2$  and  $L_2$  form a bandpass filter tuned at  $f_o$  and  $R_L$  is the load at  $f_o$ . The received signal is modeled as a voltage source  $V_a$  in series with the antenna radiation resistance  $R_a$ . The series combination of  $V_a$ ,  $R_a$ , and  $L_a$  is considered to be an ESA circuit model operating in the receive mode.

In Fig. 1,  $C(t)$  is a time-variant capacitor that can be a varactor diode modulated by a pump source at  $f_p = f_o - f_s$ . Time variation of the capacitor [9] can be simplified to:

$$C(t) = C_0(1 + 2M \cos(2\pi f_p t)) \quad (1)$$

where  $C_0$  and  $M$  are the average value of the time-domain capacitance and the modulation index, respectively. Furthermore,  $R_s$  represents the loss of the varactor diode. The mixing of the sinusoidal waveform in the signal circuit at  $f_s$  and the time modulated capacitor at  $f_p$  produces a new harmonic at  $f_o = f_p + f_s$  in the output circuit. The amplifier gain,  $G_a$ , is computed as:

$$G_a = \frac{\text{Power delivered to } R_L \text{ at } f_o}{\text{Available power from source at } f_s} = \frac{4R_a V_L^2}{R_L V_s^2} \quad (2)$$

where  $V_L$  is the voltage across the load,  $R_L$ . In [9],  $G_a$  is calculated using (2) at the center frequency of the amplifier frequency range. Gain over frequency ranges can be obtained after the same procedure as:

$$G_a = \frac{4R_a R_L}{\left| \frac{j2\pi f_s(1 - M^2)C_0 Z_{TO} Z_{TS}}{M} - \frac{M}{j2\pi f_o(1 - M^2)C_0} \right|^2} \quad (3)$$

where,

$$Z_{TO} = R_L + R_s + j2\pi f_o L_a + \frac{1}{j2\pi f_o C_2} + \frac{1}{j2\pi f_o(1 - M^2)C_0}$$

$$Z_{TS} = R_a + R_s + j2\pi f_s L_a + \frac{1}{j2\pi f_s C_1} + \frac{1}{j2\pi f_s(1 - M^2)C_0}$$

Receive antenna model

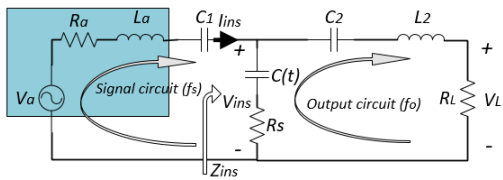


Fig. 1. The basic configuration of the up-converter parametric amplifier.

### B. Wideband Matching Technique

It is necessary to specify  $f_s$  and  $f_o$  in order to design an up-converter parametric amplifier. Therefore, as an example, we select  $f_s = 150$  MHz and  $f_o = 2050$  MHz. The values of the components for this model are given in the caption of Fig. 2. The amplifier gain is calculated using (3) for peak maximum condition ( $R_L = R_a = 19.14$ ) as a function of  $f_s$  (input signal frequency) and the outcomes are plotted in solid line (Fig. 2). As shown in this figure, the bandwidth of the output stage ( $BW = 2.42$  MHz) is nearly doubled compared to the resonator bandwidth of the input stage, which is defined as

$$\Delta f_s = \frac{f_s}{Q_s} = \frac{R_a}{2\pi L_a} \quad (4)$$

where  $Q_s$  is the unloaded quality factor of the input circuit (receive antenna). The equivalent impedance of the time-variant capacitor at  $f_s$  is defined as:

$$Z_{ins} = \frac{V_{ins}}{I_{ins}} \quad (5)$$

where  $V_{ins}$  and  $I_{ins}$  are the voltage and current of the time-varying capacitor at  $f_s$  as shown in Fig. 1. One can compute the real part of the equivalent impedance at mid-band as [9]:

$$R_{ins} = \text{Re}[Z_{ins}] = R_s + \frac{M^2}{4\pi^2 f_s f_o C_0^2 (1 - M^2)^2 (R_L + R_s)} \quad (6)$$

At this point, we can define the modified bandwidth of the input circuit resonator (after adding  $R_{ins}$ ) as:

$$\Delta f_{SL} = \frac{f_s}{Q_{SL}} = \frac{(R_a + R_{ins})}{2\pi L_a} \quad (7)$$

where  $Q_{SL}$  is the loaded quality factor of the input circuit (receive antenna). For the maximum gain condition (matched case),  $R_{ins}$  is equal to  $R_a$  resulting in  $\Delta f_{SL} = 2\Delta f_s$  which simply explains why the overall signal bandwidth is twice of the bandwidth of the unloaded input circuit resonator.

According to (6) and (7), reducing the load resistance,  $R_L$ , rises the equivalent resistance of the time variant capacitor,  $R_{ins}$ , resulting in reducing the loaded quality factor of the input circuit and thus increasing its bandwidth. Fig. 2 demonstrates the calculated amplifier gain using (3) for different  $R_L = R_a$  values. As shown in Fig. 2, reducing  $R_L$  decreases the gain of the amplifier (and flattens it), also increasing its bandwidth. Gain reduction is due to input and output circuits impedance mismatch.

Mismatch at the input circuit leads the signal to noise ratio to be reduced, resulting in the general noise figure of the receiver being degraded. However, owing to two primary factors, the general noise figure in the suggested method is still small: The antenna is a part of the amplifier circuit that allows omitting the loss of the transmission line between the antenna and the amplifier. Also, because of its reactive nature compared to the transistor counterpart which is a resistive element, the parametric amplifier is naturally a low noise device.

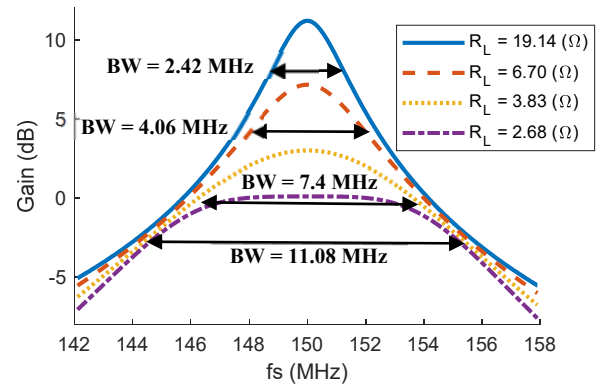


Fig. 2. Amplifier gain versus source resistance (for all graphs  $R_L = R_a$ ,  $C_1 = 0.5$  pF,  $C_2 = 0.2$  pF,  $C_0 = 4$  pF,  $M = 0.25$ ,  $R_s = 0.35$   $\Omega$ ,  $L_a = 2.55$   $\mu$ H, and  $L_2 = 31.74$  nH).

We define bandwidth improvement as the bandwidth ratio of the amplifier output over the unloaded resonator of the input circuit. ( $BW/\Delta f_s$ ). Fig. 3 shows bandwidth enhancement and amplifier gain versus  $R_L$ . As seen, the bandwidth has improved about 64 times for  $R_L = R_a = 2.68 \Omega$ , corresponding to 0 dB overall gain (the parametric amplifier gain was compensated for the mismatch loss).

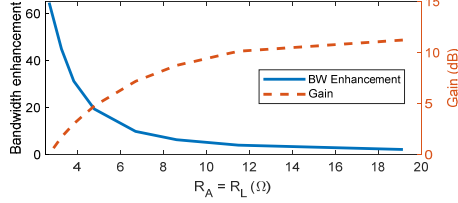


Fig. 3. Amplifier gain versus source resistance (for all graphs  $R_L = R_a$ ).

### C. Noise Considerations

The noise figure of the up-converter parametric amplifier is defined as:

$$NF = \frac{N_{out}}{N_i G_a} \quad (8)$$

where  $N_{out}$  is the output noise power delivered to the load as a result of noise generated by  $R_a$  at  $f_s$  and noise generated by  $R_s$  at  $f_s$  and  $f_o$ . The noise figure of the up-converter parametric amplifier at midband frequency was derived in [9]. We used the same method here to formulate the noise figure over the frequency ranges. Fig. 4 illustrates the noise figure for different values of  $R_L = R_a$ . As depicted, the noise figure is lower than 3 dB when  $R_L = R_a = 2.68 \Omega$  corresponding to 64 times bandwidth enhancement.

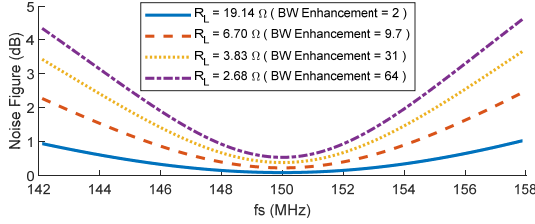


Fig. 4. Noise figure versus source resistance (for all graphs  $R_L = R_s$ ).

## III. ADS SIMULATIONS

Fig. 5 Shows ADS harmonic balance (HB) simulation setup. A series resonant circuit centered at  $f_p$  along with AC source is utilized as a pump source (Pump circuitry is included in the time-variant capacitor block in the ADS simulation). This circuit loads the signal and output circuits and detunes their resonance frequencies slightly. To retune resonance frequencies,  $L_a$  has been decreased by 0.4% while  $L_2$  has been reduced by 0.7% compared to those given in the caption of Fig. 2. All other components values remain unchanged in the ADS simulations.

The nonlinear capacitor ( $C(v) = C_0 + C_{11}v$ ) model in the ADS is used as a core element of the parametric amplifier. In accordance with the previous section,  $C_0$  and  $R_s$  are set to 4 pF and 0.35 Ω and  $C_{11}$  and pump voltage are adjusted to have  $M =$

0.25. It is worth mentioning that the values of  $C_0$ ,  $R_s$ , and  $M$  are chosen based on the datasheet of the commercially available varactor diode (SMV1413 from Skyworks Co., Ltd.).

Gain, noise figure, and phase response of ADS results are compared with analytical ones for two different values of the load resistance in Fig. 6, 7, and 8, respectively. As it is seen, ADS results are in close agreement with the analytical ones.

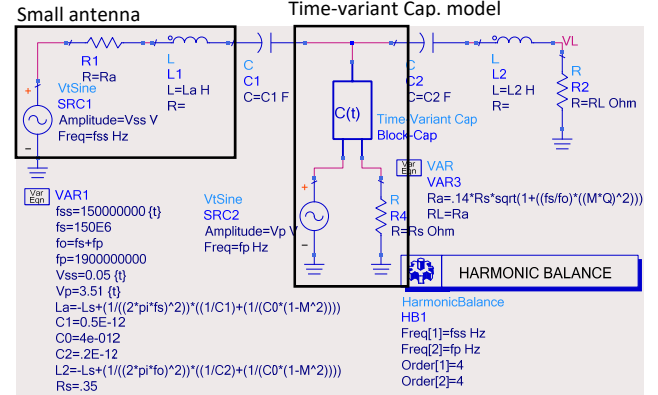


Fig. 5. ADS HB simulation setup.

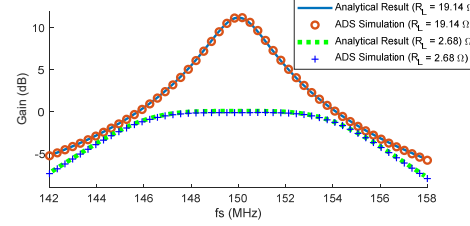


Fig. 6. Amplifier gain for  $R_a = R_L = 19.14$  and  $2.68 \Omega$ .

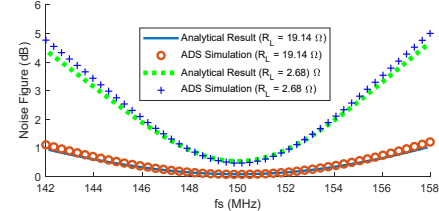


Fig. 7. Amplifier noise figure for  $R_a = R_L = 19.14$  and  $2.68 \Omega$ .

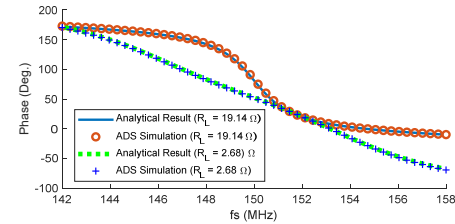


Fig. 8. Amplifier phase response for  $R_a = R_L = 19.14$  and  $2.68 \Omega$ .

## IV. BODE-FANO BOUND

Matching networks is one of the basic components of the most of RF systems. Low insertion loss and wide bandwidth are common goals in the design of matching circuits. Fano has shown that there is a trade-off between these two objectives when a purely resistive load/source has to match a complex source/load impedance that incorporates lossless LTI matching

networks. [3]. His research resulted in some integral equations related to the reflection coefficient and matching bandwidth to the values of lumped components in the complex source/load.

In the case of matching of the simple series RL circuit as a complex source to a purely resistive load, Fano's integral equations simplify as follows:

$$\int_0^\infty \ln \frac{1}{|\Gamma|} df \leq \frac{0.5}{L_a/R_a} \quad (9)$$

where  $\Gamma$  is the reflection coefficient of the matching network.  $L_a$  and  $R_a$  are components of the series RL circuit which must be matched to a pure resistance  $R_L = R_a$ . Equation (9) puts the upper limit on the area under  $\ln(1/|\Gamma|)$  over the entire frequency band for prescribed  $L_a$  and  $R_a$ . Increasing the source quality factor ( $Q_S \propto (L_a/R_a)$ ) reduces the upper limit, resulting in narrowing the maximum possible matching bandwidth of small antennas. As described in [3], considering constant value for  $\ln(1/|\Gamma|) = (\ln(1/|\Gamma|))_{\max}$  in the desired frequency range and making it zero in other frequencies leads to efficient use of the area under the integration. In this case, the maximum bandwidth of match is obtained as:

$$\Delta f_{\max} = \frac{0.5}{(L_a/R_a) \times (\ln \frac{1}{|\Gamma|})_{\max}} \quad (10)$$

Which requires a matching network with a large number of elements. For 3 dB mismatch loss ( $(\ln(1/|\Gamma|))_{\max} = 0.35$ ),  $L_a = 2.54 \mu\text{H}$ , and  $R_a = 2.68 \Omega$ , the maximum matching bandwidth is computed as  $\Delta f_{\max} = 1.5 \text{ MHz}$ . The gain function of such a network is shown in Fig. 10 (Bode-Fano unlimited case). Smaller number of elements decreases the matching bandwidth. A 4<sup>th</sup> order Chebyshev matching network has been designed for the same values of  $|\Gamma|$ ,  $L_a$ , and  $R_a$  using the method described in [3] and Fig. 9 shows ADS simulation of such a network.

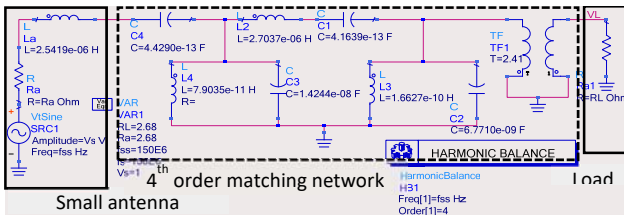


Fig. 9. LTI passive 4<sup>th</sup> order Chebyshev matching network based on Bode-Fano technique.

The gain function is calculated by ADS using  $G_{4th} = 4 \times (R_a/R_L) \times (V_L/V_s)^2$  and is plotted in Fig. 10. 4<sup>th</sup> order Chebyshev matching network results in 3 dB bandwidth of 1.25 MHz, which is slightly lower than the  $\Delta f_{\max} = 1.5 \text{ MHz}$ .

For comparison, another ADS simulation is performed without utilizing any matching circuit. In this case, the same source impedance ( $L_a = 2.54 \mu\text{H}$  and  $R_a = 2.68 \Omega$ ) is tuned using a series capacitor and is connected directly to a matched load,  $R_L = 2.68 \Omega$ . The gain of this structure (loaded resonator) is plotted in Fig. 10 which shows 3 dB bandwidth of 335.8 kHz.

The same values of  $L_a$ ,  $R_a$ , and  $R_L$  used to generate Fig. 6, 7, and 8 were implemented in our proposed matching circuitry and simulated using ADS. The ADS result for the overall gain is

shown in Fig. 10 to clarify the effectiveness of our method. As seen, 3 dB bandwidth of 10.8 MHz is achieved using the proposed technique. The 3 dB bandwidth achieved by of our technique is 7.2, 8.6, and 32 times larger than that obtained bandwidth using the Bode-Fano unlimited case, Bode-Fano 4<sup>th</sup> order case, and the loaded resonator, respectively. It is necessary to point out that, as reported in Fig. 7, the noise figure of the proposed method is lower than 3 dB in the desired frequency ranges.

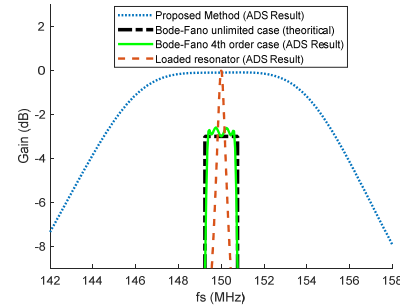


Fig. 10. Comparison between the Bode-Fano method, the proposed technique, and the loaded resonator. In all graphs, the same values for the source impedance ( $L_a$  and  $R_a$ ) and the load ( $R_L$ ) is considered.

## V. CONCLUSION

A low noise technique to increase the impedance bandwidth of the small antennas was demonstrated using theoretical formulation and simulation results. Integrating small antenna circuit model to time-variant (active) reactor enabled us to overcome the Bode-Fano bound. In future works, this theory will be applied to practical small antennas.

## REFERENCES

- [1] L. J. Chu, "Physical Limitations of Omni-Directional Antennas," *Journal of Applied Physics*, vol. 19, no. 12, pp. 1163-1175, 1948, doi: 10.1063/1.1715038.
- [2] M. Manteghi, "Fundamental Limits, Bandwidth, and Information Rate of Electrically Small Antennas: Increasing the Throughput of an Antenna Without Violating the Thermodynamic Q-Factor," *IEEE Antennas and Propagation Magazine*, vol. 61, no. 3, pp. 14-26, 2019, doi: 10.1109/MAP.2019.2907892.
- [3] R. M. Fano, "Theoretical limitations on the broadband matching of arbitrary impedances," *Journal of the Franklin Institute*, vol. 249, no. 1, pp. 57-83, 1950/01/01/ 1950, doi: [https://doi.org/10.1016/0016-0032\(50\)90006-8](https://doi.org/10.1016/0016-0032(50)90006-8).
- [4] S. Qin, Q. Xu, and Y. E. Wang, "Nonreciprocal Components With Distributedly Modulated Capacitors," *IEEE Transactions on Microwave Theory and Techniques*, vol. 62, no. 10, pp. 2260-2272, 2014, doi: 10.1109/TMTT.2014.2347935.
- [5] P. Loghmannia and M. Manteghi, "An Active Cavity-Backed Slot Antenna Based on a Parametric Amplifier," *IEEE Transactions on Antennas and Propagation*, pp. 1-1, 2019, doi: 10.1109/TAP.2019.2920236.
- [6] C. Caloz and Z.-L. Deck-Léger, "Spacetime Metamaterials," *arXiv preprint arXiv:1905.00560*, 2019.
- [7] A. Shlivinski and Y. Hadad, "Beyond the Bode-Fano Bound: Wideband Impedance Matching for Short Pulses Using Temporal Switching of Transmission-Line Parameters," *Physical Review Letters*, vol. 121, no. 20, p. 204301, 11/16/ 2018, doi: 10.1103/PhysRevLett.121.204301.
- [8] S. E. Sussman-Fort and R. M. Rudish, "Non-Foster Impedance Matching of Electrically-Small Antennas," *IEEE Transactions on Antennas and Propagation*, vol. 57, no. 8, pp. 2230-2241, 2009, doi: 10.1109/TAP.2009.2024494.
- [9] E. C. Robert, "Parametric Amplifiers," in *Foundations for Microwave Engineering*: Wiley-IEEE Press, 2001, p. 944.